HEFAT2005
4th International Conference on Heat Transfer, Fluid Mechanics and Thermodynamics
Cairo, Egypt
Paper number: RK1

LARGE EDDY SIMULATION OF TURBULENT UNCONFINED SWIRLING FLOWS

K.K.J.Ranga Dinesh, [*1] W. Malalasekera [1] , S.S. Ibrahim [2] and M.P .Kirkpatrick [3]
*Author for correspondence
[*1] Wolfson School of Mechanical and Manufacturing Engineering, Loughborough University
Loughborough, Leicestershire, LE11 3TU, UK
Email: K.K.J.Ranga-Dinesh@lboro.ac.uk, W.Malalasekera@lboro.ac.uk
[2] Department of Aeronautical and Automotive Engineering, Loughborough University
Loughborough, Leicestershire, LE11 3TU, UK
Email: S.S.Ibrahim@lboro.ac.uk
[3] School of Engineering, University of Tasmania, Private Bag 65, Hobart, 7001, Australia
Email: Michael.kirkpatrick@utas.edu.au

ABSTRACT

Swirl stabilized flames are common in many engineering applications and modeling of such flames is particularly difficult due to their recirculation and vortex characteristics. Most standard approaches such as k-e and Reynolds Stress models based Reynolds averaged Navier-Stokes (RANS) equations which work very well in other situations fail to perform well in high swirl recirculating flows. In this study a recently developed large eddy simulation (LES) code has been applied for the prediction of non reacting swirling flows experimentally tested by Al-Abdeli and Masri [1]. For the sub-grid scale closure, the localized dynamic Smagorinsky eddy viscosity model is used. Predicted results are compared with experimentally measured mean velocities, rms fluctuations and Reynolds shear stresses. The agreement between predictions and experiments are very good at most axial and radial locations, although some discrepancies exist at certain locations downstream from the burner exit plane. It is observed that great care has to be taken over the boundary conditions specification for the LES simulation of high swirl intensity recirculation flows.

INTRODUCTION

An understanding of turbulent swirling flames is important for the design of many engineering devices such as gas turbines, burners, internal combustion engines etc, and there is a clear need to develop successful predictive tools. Their recirculating standing vortex behaviour helps to improve the mixing in the flame, particularly in the shear layer region and contribute to stability through the formation of a recirculation zone. The boundary between the forward flow and the reversed flow is a region of steep velocity gradients and high intensity turbulence which promotes rapid mixing and also reduces both flame length and flame detachment which is necessary for complete combustion and stability. Recently advanced computational fluid dynamics (CFD) approaches are slowly gaining acceptance as potentially better tools for calculating practical engineering applications.

Large eddy simulation (LES) is a powerful tool for predicting complex swirling flows, due to its capability of simulating three dimensional unsteady large scale turbulent motions [2]. In LES the large scales motions in the flow are calculated explicitly while the effect of the small scales known as sub-grid scales (SGS) is modelled. In turbulent combustion the reacting phenomena occur on the scales that are typically well below to the resolution of the LES grid. Consequently some form of a sub-grid scale combustion model is also required [3]. The principal motivation of the current work is to investigate the applicability of the large eddy simulation technique to an unconfined, non-reacting swirling jet and compare the results with high quality experimental data. The test case is based on experimental measurements taken on the Sydney swirl burner [1,4]. The particular case presented here is the case N29S054 described in reference [1]. This case has a high swirl number and a range of streamwise annular velocities.

The LES code used for the simulations is the PUFFIN code [5,6,7]. The Smagorinsky eddy viscosity model [8] with the localized dynamic procedure of Piomelli and Liu [9] is used for sub-grid scale turbulence modelling. This model calculates the Smagorinsky model coefficient automatically by using the information contained in the resolved field. In this paper, we compare LES and experimental results for the mean velocities, rms fluctuations and Reynolds shear stresses.

NOMENCLATURE

$C(x,t)$	*Smagorinsky model coefficient*
G	*Filter width function*
P	*Pressure*
r	Radial distance (mm)
Re_s	Swirling annulus Reynolds number
S	Swirl number

S_g Geometric swirl number

S_{ij} Strain rate tensor

x Axial position (mm)

Greek Letters

$\bar{\Delta}$ Grid filter width

μ Dynamic viscosity

μ_{sgs} Sub-grid scale dynamic viscosity

τ_{ij} Sub-grid scale stress

ρ Density (kg/m^3)

EXPERIMENTAL SETUP

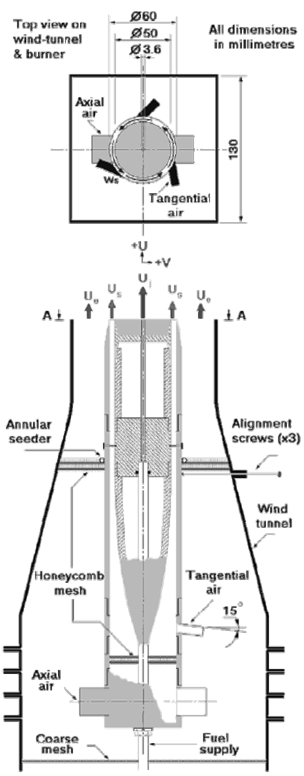

Figure 1: Schematic plot of the experimental rig

The experimental setup is shown schematically in Fig 1. The test rig consists of a 50mm cylindrical bluff body with 3.6mm diameter central fuel jet. Surrounding the cylindrical bluff body is a 60mm diameter annulus machined down to 0.2mm thickness at the exit plane. The centre of the fuel jet is taken as the geometric centre line of the flow where r=0 and x=0. The test is housed in a secondary co-flow wind tunnel with a square cross section 130mm sides. Swirl is introduced aerodynamically into the primary (axial) air stream by using three tangential (air) swirl ports at a distance 300mm upstream of the burner exit. The level of swirl is represent by the swirl number defined as the ratio between the axial flux of swirl momentum to the axial flux of axial momentum multiplied by a characteristic radius R such that

$$S = \frac{\int_0^R \langle u \rangle \langle w \rangle r^2 dr}{R \int_0^R \langle u \rangle^2 dr}.$$

The bulk jet velocity of the fuel inlet $< U_j >$, the bulk and tangential velocity of the primary air stream $< U_s >$ and $< W_s >$ are the three parameters which control the stability characteristics and physical properties of the flow. The co-flowing air stream $< U_e >$ may also influence the flow. The geometric swirl number S_g is defined as a ratio of integrated (bulk) tangential to axial air velocities (W_s / U_s). The swirl number can be varied by changing the relative flow rates of tangential and axial air in the primary stream. The Reynolds number of the annulus air stream is defined in terms of bulk axial velocity and the outer radius of the annulus.

Flow Case	Flow	U_s (m/s)	W_s (m/s)
N29S054	Isothermal	29.7	16
U_j (m/s)	U_e (m/s)	S_g	Re
66	20	0.54	59,000

Table 1: Flow conditions and control parameters

GOVERNING EQUATIONS AND MODELLING

In the LES technique the solution space is partitioned into resolved and unresolved scales, typically through the application of a spatial filter. A filter G is applied to the flow variable f with filter width $\bar{\Delta}$ such that

$$\bar{f}(x) = \int f(x) G(x - x', \bar{\Delta}) dx'$$

Application of a spatial filter to the Navier-Stokes equations for non-reacting isothermal turbulent flows gives

$$\frac{\partial \bar{\rho}}{\partial t} + \frac{\partial (\overline{\rho u}_j)}{\partial x_j} = 0$$

$$\frac{\partial \overline{\rho u_i}}{\partial t} + \frac{\partial (\overline{\rho u}_i \bar{u}_j)}{\partial x_j} = -\frac{\partial \bar{P}}{\partial x_j} + \frac{\partial (2 \mu \bar{S}_{ij})}{\partial x_j} + \bar{\rho} g_i - \frac{\partial \tau_{ij}}{\partial x_j}$$

For the isothermal case presented here, density is constant and the flow may be assumed to be incompressible. We note that in application of the code to reacting flow cases, these equations are replaced by equations written in a Favre-filtered form, with an anelastic approximation used to account for density variations.

As a result of the spatial filtering the sub-grid scale stress τ_{ij} is introduced into the momentum equations. This sub-grid scale stress $\tau_{ij} = \overline{\rho}(\overline{u_i u_j} - \overline{u}_i \overline{u}_j)$ is modelled by using the Smagorinsky eddy viscosity model [5]

$$\tau_{ij} - \frac{1}{3}\delta_{ij}\tau_{kk} = -2\overline{\mu}_{sgs}\overline{S}_{ij}.$$

The eddy viscosity μ_{sgs} is a function of filter size and the strain rate such that

$$\mu_{sgs} = \overline{\rho} C \overline{\Delta}^2 \left|\overline{S}\right|.$$

The localized dynamic procedure of Piomelli and Liu [9] is used to calculate the model coefficient C dynamically by using the relation

$$C = -\frac{(L_{ij} - 2\overline{C^* B_{ij}})A_{ij}}{2A_{kl}A_{kl}}.$$

Where C^* is the previous time step value of C and $\alpha = \overline{\overline{\Delta}}/\overline{\Delta}$,

$$A_{ij} = \alpha^2 \overline{\Delta}^2 \left|\overline{\overline{S}}\right| \overline{\overline{S}}_{ij},\ B_{ij} = \overline{\Delta}^2 \left|\overline{S}\right| \overline{S}_{ij},\ L_{ij} = \overline{\overline{u}_i \overline{u}_j} - \overline{\overline{u}}_i \overline{\overline{u}}_j.$$

COMPUTATIONAL METHOD

The large eddy simulation code PUFFIN [5,6] is used to solve the equations presented above. The filtered flow equations are discretised in space by using the finite volume approach. All spatial derivatives in momentum and pressure correction equations are approximated by second order central differences. The time derivatives are approximated by a third order hybrid Adams-Bashforth/Adams-Moulton (ABAM) scheme. A Bi-Conjugate Gradient Stabilised (BICGStab) solver is used to solve the system of algebraic equations resulting from the discretisation. Further details of the numerical schemes can be found in [6].

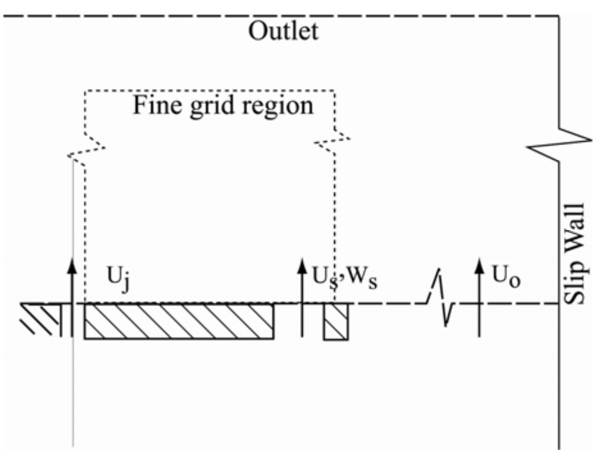

Figure 2: Computational domain

Figure 2 shows the computational domain for the simulation. The numerical grid employed in the simulation has $120\times120\times100$ grid nodes in *x*, *y* and *z* directions respectively. The grid is expanded outwards from the centre with an expansion ratio of 1.05 in the *x* and *y* directions and also expanded into the *z* direction with an expansion ratio of 1.01. Free slip boundary condition is applied on the sides of the domain while zero normal gradient outlet boundary condition is applied to the top of the domain. Correct representation of inflow turbulence is an important issue for LES. Our initial calculations showed that LES results are sensitive to inlet boundary conditions. We have used a simple method to generate the inflow boundary conditions by adding random fluctuations to the measured mean velocity profiles such that the amplitude of the random fluctuation of each velocity component is rescaled to match the measured variance of the velocity fluctuations.

RESULTS AND DISCUSSION

Comparison of the LES computation and experimental measurements [1,4] are presented in this section. The experimental measurements for mean velocities, turbulent intensities and Reynolds shear stresses are available at eight different downstream axial positions (*x*) from the burner exit plane. Figures below show the comparison of the LES and experimental results for the test case known as N29S054 which operates at a swirl number 0.54. In the following figures the solid lines indicate the LES results and circles indicate the experimental measurements.

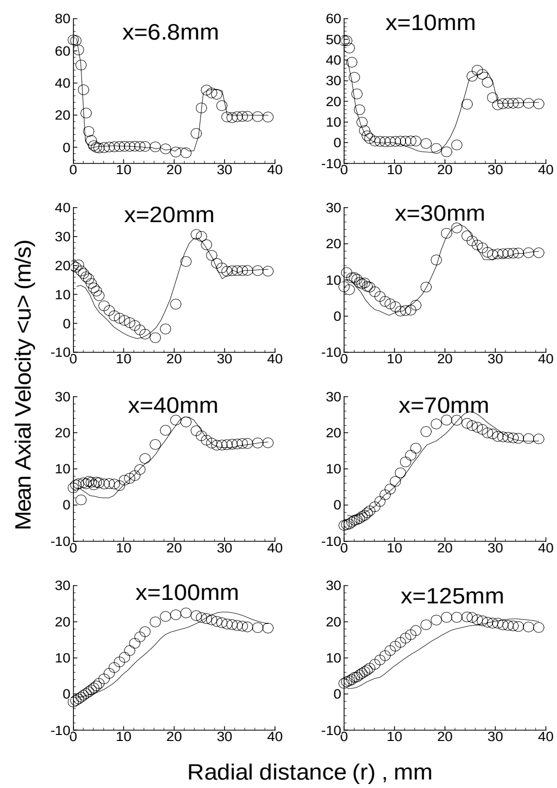

Figure 3: Radial profiles for the mean axial velocity

Figures (3), (4) and (5) show the comparison between measured and computed radial profiles for mean axial, radial and swirling velocities at eight different downstream axial measurement positions ranging from x=6.8mm to x=125mm. The overall agreement between experiments and calculations for the mean axial and swirling velocities is seen to be very good at most measurement positions. There are some discrepancies between the results for the mean radial velocities. This might be related to the grid resolution in that particular recirculation zone. A positive to negative change in mean axial velocity indicates the development of a recirculation region. The first recirculation zone develops at about 30mm above from the ceramic faced bluff body. A special feature of this flow case is the existence of a second recirculation zone which stagnates on the jet centerline at x=50mm and 100mm. This zone of air takes on the form of a closed bubble and has peak mean axial velocity of about $< u >$ = -6 m/s occurring on the centre line at x=80mm. The predictions have captured both recirculation zones (Fig. 3). The length of each recirculation zones may be obtained from contour plots of axial velocity (not shown here in the interest of brevity). The calculated lengths shows slight discrepancies with the measured lengths, in particular the calculated length of the second recirculation zone is less than that measured in experiments.

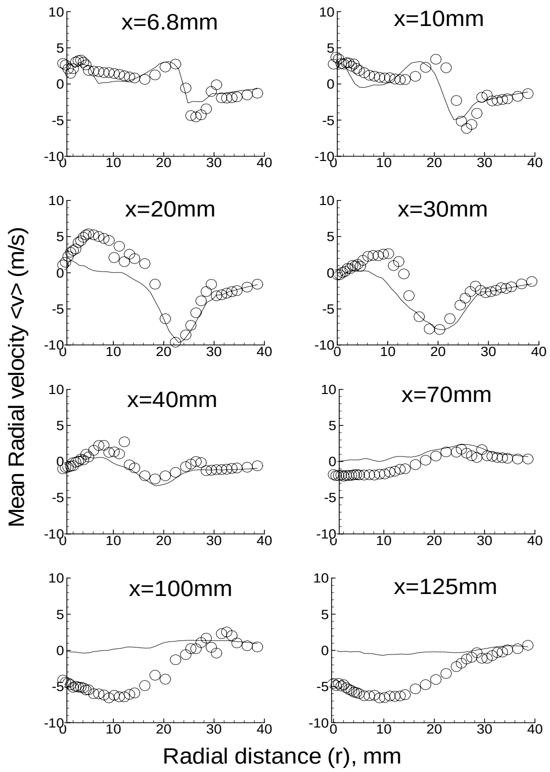

Figure 4: Radial profiles for the mean radial velocity

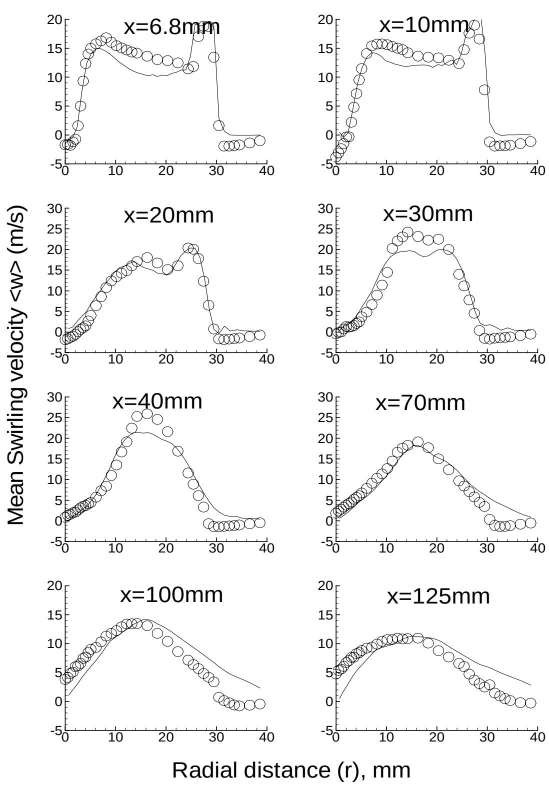

Figure 5: Radial profiles for the mean swirling velocity

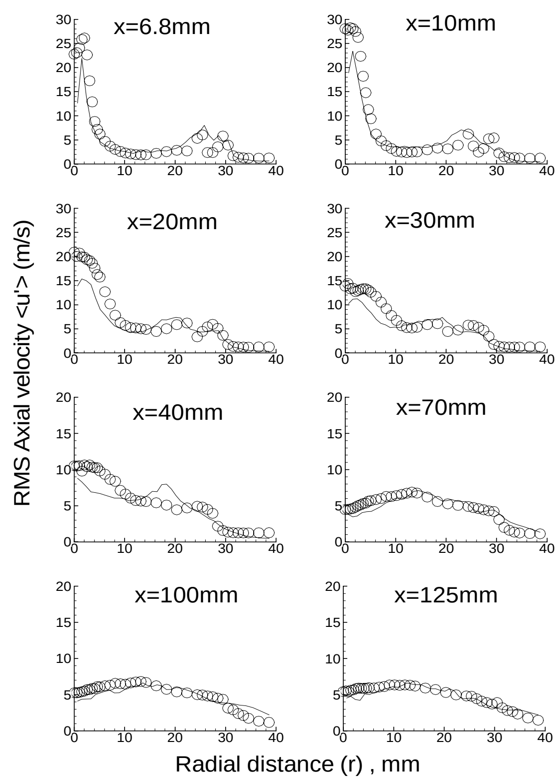

Figure 6: Radial profiles for the rms axial velocity

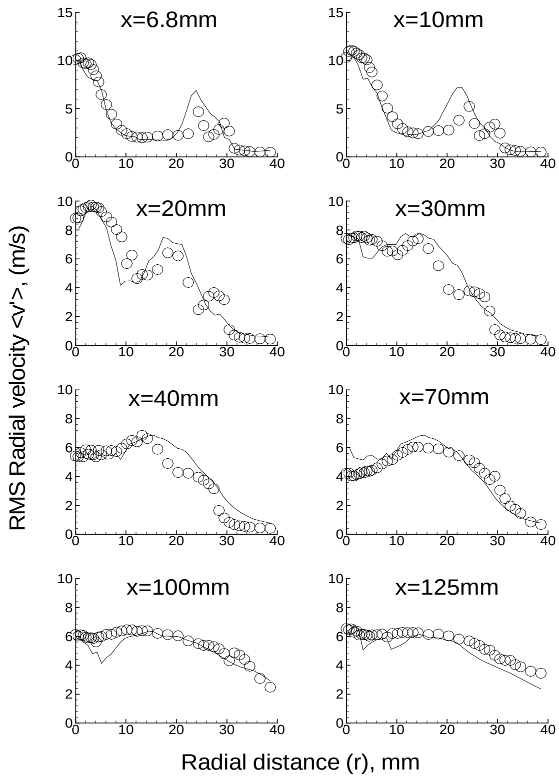

Figure 7: Radial profiles for the rms radial velocity

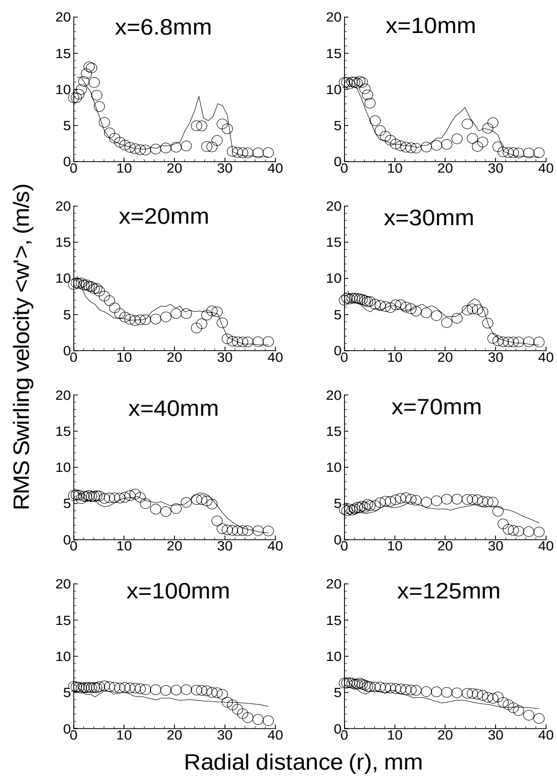

Figure 8: Radial profiles for the rms swirling velocity

Figures (6), (7) and (8) show comparison between measured and computed rms fluctuations of axial, radial and swirling velocities. The qualitative and quantitative agreement between experimental and computational results is very good at most of the downstream axial positions. It should be noted that there are some discrepancies at some axial and radial positions for the rms radial and swirling velocities. We believe that use of a finer grid could improve these minor discrepancies. It is also noted that LES only gives the resolved part of the rms fluctuations.

Figures (9) and (10) show the comparison between the measured and computed Reynolds shear stresses for $<u'v'>$ and $<u'w'>$. The comparison shows good agreement for most of the downstream axial positions. However LES under-predicts the $<u'v'>$ stresses at some axial positions such as x=40mm. Additionally the stresses $<u'w'>$ are higher near to the jet and in the annulus area (radial position =25-30mm. These stresses continue to diminish in magnitude further downstream in the flow. This is due the formation of the downstream recirculation zone leading to higher velocity gradients and stresses. Thus the downstream part of the flow can expect improved mixing rates from both recirculation and shear stresses. It can be seen from the above comparison that LES shows very good predictions overall and LES appear to be a very successful technique for the modeling of swirling flows. The ability of LES to predict velocity fluctuations as well as Reynolds shear stress is the great advantage where correct representation of the turbulence field is important for practical combustion applications. We have conducted parametric studies to understand the sensitivity of boundary conditions on the LES results. It appears that the method we have used here gives good comparison with experimental data.

CONCLUSION

This paper mainly concerns the large eddy simulation of a non-reacting isothermal strongly swirling flow. The test case used has a swirl number 0.54 and is based on experimental measurements taken by Al-Abdeli and Masri [1] on the Sydney swirl burner. With sufficient grid resolution and suitable inflow and outflow boundary conditions, the LES method successfully predicts the experimentally measured mean velocity, turbulence intensity and the Reynolds shear stresses. A special feature of this simulated test case is the existence of two recirculation zones. The first takes the form of an open toroid near to the ceramic bluff body, while the second recirculation zone stabilizes further downstream and takes on the shape of closed bubble shaped vortex. Such recirculating flow features can be attributed to vortex breakdown. Our LES attempt capture these important flow features. The comparison of predicted mean flow velocities, rms fluctuations and Reynolds shear stresses with measured experimental data show very good agreement. Given the complexity of the flow situation LES certainly appear to be a promising technique. We intend to extend these studies to include combustion.

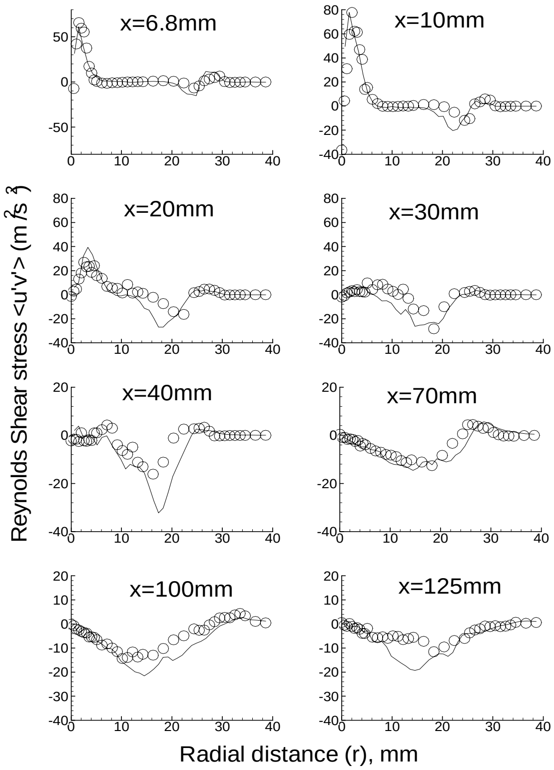

Figure 9: Radial profiles for the Reynold shear stress

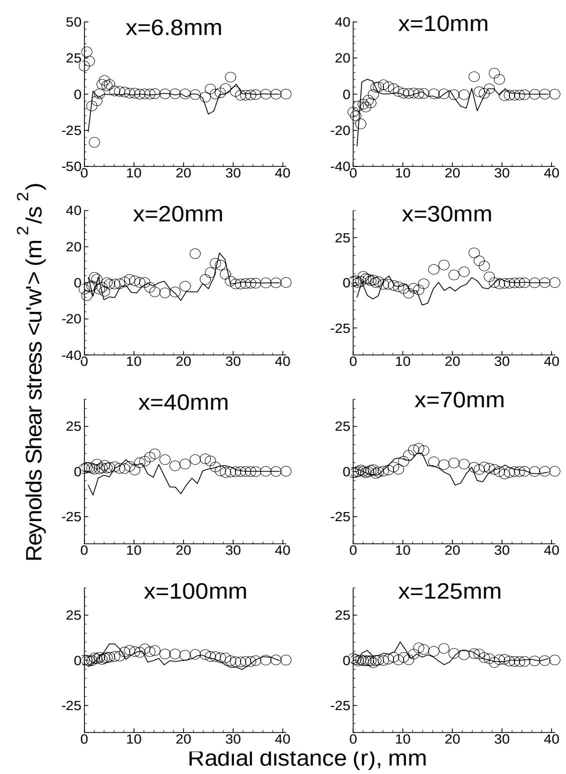

Figure 10 : Radial profiles for the Reynolds shear stress

REFERENCES

[1] Al-Abdeli, Y.M, Masri, A.R., 2003, "Recirculation and flow field regimes of unconfined non-reacting swirling flow," Experimental and Thermal Sciences, vol 23, pp. 655-665.

[2] Pierce, C.D. and Moin, P., 1998, "Method for generating equilibrium swirling inflow conditions," AIAA Journal, vol 36, pp. 1325-1327.

[3] Branley, N., 1999, "Large eddy simulation of Turbulent non-premixed flames," PhD Thesis, Department of Chemical Eng, Imperial college of Science and Technology, UK.

[4] Al-Abdeli, Y.M, 2003, "Experiments in Turbulent swirling non-premixed flame and isothermal flows," PhD Thesis, School of Aerospace Mechanical and Mechatronic Eng, University of Sydney, Australia.

[5] Kirkpatrick, M.P., 2002, "Large eddy simulation code for industrial and environmental flows," PhD Thesis, School of Aerospace Mechanical and Mechatronic Eng, University of Sydney, Australia.

[6] Kirkpatrick, M.P, Armfield, S.W, Kent, J.H, 2003, "A representation of curved boundaries for the solutions of the Navier-Stokes equations on a staggered three dimensional Cartesian grid," Journal of Computational Physics,vol 104, pp1-36.

[7] Kirkpatrick, M.P, Armfield, S.W, Masri, A.R and Ibrahim, S.S, 2003, "Large eddy simulation of a propagating premixed flame," Flow Turbulence and Combustion, vol 70, pp. 1-19

[8] Smagorinsky, J., 1963, "General circulation experiments with the primitive equations," Monthly Weather Review, 91, pp.99- 164.

[9] Piomelli, U. and Liu, J., 1995, "Large eddy simulation of channel flows using a localized dynamic model," Physics of fluids, vol 7, pp. 839-848.

[10] Germano, M. ,Piomelli, U., Moin, P. and Cabot, W.H., 1991, " Dynamic subgrid eddy viscosity model," Physics of fluids, vol. 3, pp. 1760-1765.

[11] Bear, J.M. and Chigier, N.A., 1972, "Combustion Aerodynamics," Wiley, New-York.